ARCHIVIO ISTITUZIONALE
DELLA RICERCA

Alma Mater Studiorum Università di Bologna
Archivio istituzionale della ricerca

How to handle negative interest rates in a CIR framework

This is the submitted version (pre peer-review, preprint) of the following publication:

Published Version:
Di Francesco M., Kamm K. (2022). How to handle negative interest rates in a CIR framework. SEMA JOURNAL, 79(4), 593-618 [10.1007/s40324-021-00267-w].

Availability:
This version is available at: https://hdl.handle.net/11585/916044 since: 2023-02-18

Published:

DOI: http://doi.org/10.1007/s40324-021-00267-w

Terms of use:

Some rights reserved. The terms and conditions for the reuse of this version of the manuscript are specified in the publishing policy. For all terms of use and more information see the publisher's website.

This item was downloaded from IRIS Università di Bologna (https://cris.unibo.it/).
When citing, please refer to the published version.

(Article begins on next page)

17 September 2026

How to handle negative interest rates in a CIR framework

Marco Di Francesco* Kevin Kamm†

June 8, 2021

arXiv:2106.03716v1 [q-fin.TR] 7 Jun 2021

Abstract

In this paper, we propose a new model to address the problem of negative interest rates that preserves the analytical tractability of the original Cox-Ingersoll-Ross (CIR) model without introducing a shift to the market interest rates, because it is defined as the difference of two independent CIR processes. The strength of our model lies within the fact that it is very simple and can be calibrated to the market zero yield curve using an analytical formula. We run several numerical experiments at two different dates, once with a partially sub-zero interest rate and once with a fully negative interest rate. In both cases, we obtain good results in the sense that the model reproduces the market term structures very well. We then simulate the model using the Euler-Maruyama scheme and examine the mean, variance and distribution of the model. The latter agrees with the skewness and fat tail seen in the original CIR model. In addition, we compare the model's zero coupon prices with market prices at different future points in time. Finally, we test the market consistency of the model by evaluating swaptions with different tenors and maturities.

Keywords: CIR model, Negative interest rates, Calibration, Forecasting and simulation, Riccati Equations.

Acknowledgements: This project has received funding from the European Union's Horizon 2020 research and innovation programme under the Marie Sklodowska-Curie grant agreement No 813261 and is part of the ABC-EU-XVA project.

*UnipolSai Assicurazioni, via Stalingrado 45, Bologna, Italy, **e-mail**: marco.difrancesco@unipolsai.com

†Dipartimento di Matematica, Università di Bologna, Bologna, Italy. **e-mail**: kevin.kamm@unibo.it

The views expressed in this note are the only responsibility of the author and do not represent in any way those of author's current employer. All errors are the only responsibility of the author.

1. Introduction

The Cox-Ingersoll-Ross model (hereafter referred to as CIR model) has been regarded as the reference model in interest rate modeling by both practitioners and academics for several decades, not only because of its analytical tractability as an affine model, but also because of its derivation from a general equilibrium framework (see for example [6]), among other reasons. The well-known feature of the CIR model that ultimately led to this paper is that interest rates never become negative. This long-standing paradigm of non-negative interest rates made the CIR model and its extensions one of the most appropriate models for interest rate modeling.

Today, however, negative interest rates are very common and thus the need for models that can handle this paradigm shift is highly desirable, provided that they have as few shortcomings as possible compared to the original CIR models.

In this paper, we present a very simple and effective idea how this can be realized by modeling interest rates as the difference of two independent CIR processes, which—to the best of our knowledge—has not been considered yet.

We will propose a term structure in the risk-neutral world suitable for the difference of two independent affine processes and obtain a pricing formula for default-free zero-coupon bonds by deriving the associated Riccati equations arising from this no-arbitrage framework. In the special case of two CIR processes we will then solve the Riccati equations explicitly, which preserves the analytical tractability of its non-negative interest rate counterpart.

Afterwards, we will show some numerical experiments to demonstrate the merits of this approach in practice.

Let us consider the following affine dynamics

$$\begin{cases} dx(t) = (\lambda_x(t)x(t) + \eta_x(t))\,dt + \sqrt{\gamma_x(t)x(t) + \delta_x(t)}dW_x(t) \\ x(0) = x_0, \end{cases} \tag{1.1}$$

$$\begin{cases} dy(t) = (\lambda_y(t)y(t) + \eta_y(t))\,dt + \sqrt{\gamma_y(t)y(t) + \delta_y(t)}dW_y(t) \\ y(0) = y_0, \end{cases} \tag{1.2}$$

where henceforth throughout the whole paper W_y and W_x are two independent standard Brownian motions on a stochastic basis $\left(\Omega, \mathcal{F}, (\mathcal{F}_t)_{t\in[0,T]}, \mathbb{Q}\right)$, $\mathbb{Q}$ is a martingale measure and $T > 0$ is a finite time horizon. The initial values $x_0,\ y_0 \in \mathbb{R}$ are real-valued constants and the coefficients $\lambda_z, \eta_z, \gamma_z, \delta_z,\ z \in \{x, y\}$, are all real-valued deterministic functions, such that (1.1) and (1.2) are well-defined.

Furthermore, let the the instantaneous short-rate process be given by

$$r(t) \coloneqq x(t) - y(t). \tag{1.3}$$

In the case where $y \equiv 0$, this reduces to the standard affine one-factor short rate model class. If additionally $\delta_x(t) \equiv 0$, $\lambda_x(t) \equiv -k_x$ $\eta_x(t) \equiv k_x\theta_x$ and $\gamma_x(t) \equiv \sigma_x^2$, where $k_x, \sigma_x, \theta_x \in \mathbb{R}_{\geq 0}$,

it reduces to the standard CIR model

$$dx(t) = k_x(\theta_x - x(t))dt + \sigma_x\sqrt{x(t)}dW_x(t), \tag{1.4}$$

which lets (1.3) preserve all the features of a standard CIR model in a non-negative interest rate setting.

1.1. Description of the main results

The main result consists of two main parts. First of all, we derive the zero-coupon bond price for (1.3) in the case of the difference of (1.1) and (1.2) being two independent CIR processes as in (1.4). Secondly, we provide numerical experiments to demonstrate the features of this model in Section 3.

Theorem 1.1. *Let* $\left(\Omega, \mathcal{F}, (\mathcal{F}_t)_{t\in[0,T]}, \mathbb{Q}\right)$ *be a stochastic basis, where* $\mathbb{Q}$ *is a martingale measure,* $T > 0$ *a finite time horizon and let the* σ*-algebra* $(\mathcal{F}_t)_{t\in[0,T]}$ *fulfill the usual conditions and support two independent standard Brownian motions* W_x *and* W_y*.*

The price of a zero-coupon bond in the model $r(t) = x(t) - y(t)$ *with* x *and* y *being two independent CIR processes as in (1.4) is given by*

$$P(t,T) = A_x(t,T)e^{-B_x(t,T)x(t)}A_y(t,T)e^{B_y(t,T)y(t)}, \tag{1.5}$$

where $t \leq T$ *and for* $z \in \{x, y\}$

$$\begin{aligned} A_z(t,T) &= \left(\frac{\phi_1^z e^{\phi_2^z(T-t)}}{\phi_2^z\left(e^{\phi_1^z(T-t)} - 1\right) + \phi_1^z}\right)^{\phi_3^z} \\ B_z(t,T) &= \frac{e^{\phi_1^z(T-t)} - 1}{\phi_2^z\left(e^{\phi_1^z(T-t)} - 1\right) + \phi_1^z} \end{aligned} \tag{1.6}$$

with $\phi_i^z \geq 0$*,* $i = 1, 2, 3$*,* $z \in \{x, y\}$*, such that the Feller condition* $2k_z\theta_z \geq \sigma_z^2$ *is satisfied and*

$$\begin{aligned} \phi_1^x &= \sqrt{k_x^2 + 2\sigma_x^2}, \qquad \phi_2^x = \frac{k_x + \phi_1^x}{2}, \qquad \phi_3^x = \frac{2k_x\theta_x}{\sigma_x^2} \\ \phi_1^y &= \sqrt{k_y^2 - 2\sigma_y^2}, \qquad \phi_2^y = \frac{k_y + \phi_1^y}{2}, \qquad \phi_3^y = \frac{2k_y\theta_y}{\sigma_y^2}. \end{aligned} \tag{1.7}$$

The technical part of the proof is quite standard and referred to Appendix A with a description for deriving this result in Section 2. Formula (1.5) will provide the necessary ingredient for the numerical experiments in Section 3 to calibrate the model to the market term structure. In Section 3 we will perform several experiments at two different dates 30/12/2019 and 30/11/2020, where negative interest rates are observed in the market to uncover the features of this model.

1.2. Review of the literature and comparison

There is a vast literature on interest rate modeling, among these for example the comprehensive works of [2], [5] and [11], which we cannot cover to its full extent in this small review. The most popular approach in modern interest rate modeling is the direct modeling of short rates $r(t)$ under a risk-neutral measure $\mathbb{Q}$ inspired by no-arbitrage arguments, especially, because the price at time $t > 0$ of a contingent claim with payoff H_T, $T > t$, under the risk-neutral measure is given by (cf. [22])

$$H_t = E_t^{\mathbb{Q}}[e^{-\int_t^T r(s)ds} H_T], \tag{1.8}$$

where $E_t^{\mathbb{Q}}$ denotes the conditional expectation with respect to some filtration $\mathcal{F}_t$ under measure $\mathbb{Q}$. In particular, choosing $H_T := P(T,T) = 1$, where $P(t,T)$ denotes a zero-coupon bond, gives rise to a convenient way to calibrate a short rate model to the market term structure, which we will utilize for our approach as well.

Starting with the pioneering works of Merton [17] in 1973 and Vasicek [23] in 1977, many one-factor short rate models were introduced, see [5] for a detailed overview. Among all, a model that has had a particular importance in the past, equally among both practitioners and academics, is the well-known CIR model, proposed by Cox, Ingersoll & Ross in [7]. It provides the basis for this paper and is a generalization to the Vasicek model by introducing a non-constant volatility given by (1.4).

Clearly, the square root term precludes the possibility of negative interest rates and under the assumption of the Feller-condition $2k\theta \geq \sigma^2$, see for instance [14], the origin is inaccessible. These two properties combined with its analytical tractability make the CIR model well-suited for a non-negative interest rate setting.

There is a rich literature on extensions to the classical CIR model in order to obtain more sophisticated models, which could fit the market data better, allowing to price interest rate derivatives more accurately. For example, Chen in [1] proposed a three-factor model; Brigo and Mercurio in [5] proposed a jump diffusion model (JCIR). In order to include time dependent coefficients in (1.4), Brigo and Mercurio in [4] proposed to add a deterministic function into equation (1.4). This model, called CIR++, is able to fit the observed term structure of interest rates exactly, while preserving the positivity of the process $r(t)$. Brigo and El-Bachir in [3] generalized the CIR++ model by adding a jump term described by a time-homogeneous Poisson process and Brigo and Mercurio in [5] studied the CIR2++ model. Another way to generalize the CIR model by including time dependent coefficients in equation (1.4) was introduced by Jamshidian in [13] and Maghsoodi in [15], which are known as extended CIR models.

But in the last decade the financial industry encountered a paradigm shift by allowing the possibility of negative interest rates, making the classical CIR model unsuitable.

One way to handle the challenges entailed by negative interest rates is to use Gaussian models with one or more factors, such as the Hull and White model (see [12]), which also has a very good analytical tractability. A generalization of these models with a good calibration

to swaption market prices was found in [9], while Mercurio and Pallavicini in [16] proposed a mixing Gaussian model coupled with parameter uncertainty.

But the glamor of the CIR model is still alive even in the current market environment with negative interest rates. Orlando et al. suggest in several papers (cf. [19], [20] and [21]) a new framework, which they call CIR# model, that fits the term structure of interest rates. Additionally, it preserves the market volatility, as well as the analytical tractability of the original CIR model. Their new methodology consists in partitioning the entire available market data sample, which usually consists of a mixture of probability distributions of the same type. They use a technique to detect suitable sub-samples with normal or gamma distributions. In a next step, they calibrate the CIR parameters to shifted market interest rates, such that the interest rates are positive, and use a Monte Carlo scheme to simulate the expected value of interest rates.

In this paper, however, we introduce a new methodology for handling the challenges arising from negative interest rates. In our model, the instantaneous spot rate is defined as the difference between two independent classical CIR processes, which allows the preservation of the analytical tractability of the original CIR model without introducing any shift to the market interest rates.

The paper is organized as follows. In Section 2 we introduce the model in a general affine model setup and describe our main result Theorem 1.1. We will derive the Riccati equations associated with the proposed term structure suitable for the difference of two independent affine processes and solve those explicitly in a CIR framework.

After that, in Section 3, we will conduct some numerical experiments. First, we calibrate our model via (1.5) to the market data at 30/12/2019 and 30/11/2020 in Section 3.2. Subsequently, we simulate the model by using the Euler-Maruyama scheme in Section 3.3 and study the mean, variance and distribution of the model in Section 3.4. Then we test how the calibrated model performs when pricing zero-coupon bonds at future times in Section 3.5 and conclude our numerical tests by pricing swaptions in Section 3.6. Finally, we summarize the results of the paper in Section 4 and discuss possible extensions for future research.

2. A model for negative interest rates

We will now describe how Theorem 1.1 can be derived. As aforementioned, we consider all dynamics under the risk-neutral measure $\mathbb{Q}$ and give now a heuristic argument, why it makes sense to choose the term structure in Theorem 1.1 as in (1.5).

Suppose, that $x(t)$ and $y(t)$ are both independent affine processes. Then the the price of a zero-coupon bond for each of them separately (cf. [5] p. 69) is given by

$$P(t,T) = E_t^{\mathbb{Q}}\left[e^{-\int_t^T z(s)ds}\right] = A_z(t,T)e^{-B_z(t,T)z(t)}, \tag{2.1}$$

where $z \in \{x, y\}$ and $E_t^{\mathbb{Q}}$ denotes the conditional expectation with respect to $\mathcal{F}_t$ under the

measure $\mathbb{Q}$. Now, consider $r(t) = x(t) - y(t)$, then we have by linearity and independence

$$P(t,T) = E_t^{\mathbb{Q}}\left[e^{-\int_t^T r(s)ds}\right] = E_t^{\mathbb{Q}}\left[e^{-\int_t^T (x(s)-y(s))ds}\right] = E_t^{\mathbb{Q}}\left[e^{-\int_t^T x(s)ds}\right] E_t^{\mathbb{Q}}\left[e^{\int_t^T y(s)ds}\right].$$

If we concentrate in (2.1) only on the right-hand side, it would make sense for two independent processes x and y that we can apply these formulas with a change of sign in front of B_y, leading to

$$P(t,T) \stackrel{!}{=} A_x(t,T)e^{-B_x(t,T)x(t)}A_y(t,T)e^{B_y(t,T)y(t)}.$$

In the following Lemma we will make this argument rigorous.

Lemma 2.1. *Let everything be as in Theorem 1.1 but let $x(t)$ and $y(t)$ follow the general affine dynamics described in (1.1) and (1.2).*

Then, the price of a Zero-coupon bond is given by

$$P(t,T) = E_t^{\mathbb{Q}}\left[e^{-\int_t^T r(s)ds}\right] = A_x(t,T)e^{-B_x(t,T)x(t)}A_y(t,T)e^{B_y(t,T)y(t)}, \tag{2.2}$$

where A_z and B_z, $z \in \{x,y\}$, are deterministic functions and are a classical solution to the following system of Riccati equations

$$\begin{cases} -1 - B_x(t,T)\lambda_x(t) - (\partial_t B_x)(t,T) + \frac{1}{2}B_x^2(t,T)\gamma_x(t) = 0, & B_x(T,T) = 0 \\ -B_x(t,T)\eta_x(t) + \frac{1}{2}B_x^2(t,T)\delta_x(t) + \partial_t(\log A_x)(t,T) = 0, & A_x(T,T) = 1 \\ 1 + B_y(t,T)\lambda_y(t) + (\partial_t B_y)(t,T) + \frac{1}{2}B_y^2(t,T)\gamma_y(t) = 0, & B_y(T,T) = 0 \\ B_y(t,T)\eta_y(t) + \frac{1}{2}B_y^2(t,T)\delta_y(t) + \partial_t(\log A_y)(t,T) = 0, & A_y(T,T) = 1. \end{cases} \tag{2.3}$$

The proof of this Lemma is referred to Appendix A. The independence of x and y ensures that the Riccati equations for A_x and B_x are decoupled from the ones for A_y and B_y, making it possible to use the existing literature on explicit solutions in the context of short rate models to construct easily a solution for our difference process (1.3) in the case where x (1.1) and y (1.2) are CIR processes.

Remark 2.2. One can immediately use Lemma 2.1 and the ideas in Appendix A to construct solutions to other popular one-factor affine short rate models, where an explicit solution is available, e.g. the Vasicek model, provided that x and y are independent.

Introducing dependence between x and y suggests a coupling of A_x and B_x to A_y and B_y and might have an impact on the analytical tractability, but is left for future research.

It is well-known that, under the conditions $2k_z\theta_z \geq \sigma_z^2$, $z \in \{x,y\}$, the processes $x(t)$ and $y(t)$ are strictly positive for every $t \geq 0$ (see for instance [7] or [14]). We underline that even if the processes $x(t)$ and $y(t)$ are strictly positive, the instantaneous spot rate $r(t)$ could be negative since it is defined as the difference of $x(t)$ and $y(t)$ for every $t > 0$, which is illustrated in Figure 1 together with several percentiles of $r(t)$.

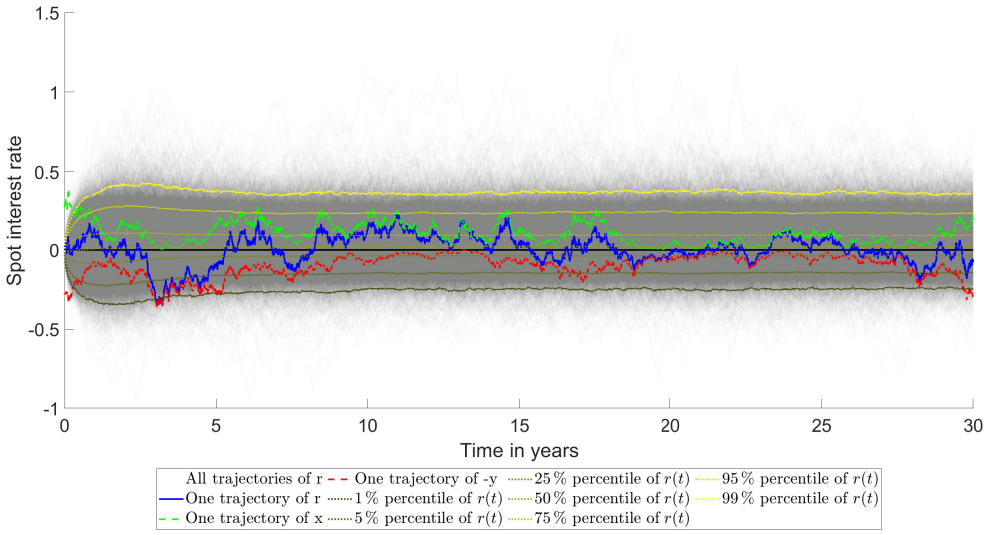

Figure 1.: An example of a trajectory with negative interest rates $r = x - y$ and its decomposition in x and $-y$, obtained with the market data on 30/12/2019 and parameters given in Table 2.

3. Numerical tests

We will now perform some numerical experiments in our model. In Section 3.1 we will briefly discuss the market data, which we will use to perform all numerical tests in the subsequent sections. Afterwards, we will describe the calibration procedure of our model to the zero-coupon curves at 30/12/2019 and 30/11/2020 in Section 3.2. This is followed by a short subsection on simulating the model with the Euler-Maruyama scheme in Section 3.3 and we investigate the mean, variance and distribution of the short rate model in Section 3.4. In Section 3.5 we price zero-coupon bonds at future dates and compare the results to the market prices. Last but not least, Section 3.6 will show results on pricing swaptions in our model.

We used for the calculations `Matlab 2021a` with the (Global) Optimization Toolbox running on Windows 10 Pro, on a machine with the following specifications: processor Intel(R) Core(TM) i7-8750H CPU @ 2.20 GHz and 2x32 GB (Dual Channel) Samsung SODIMM DDR4 RAM @ 2667 MHz.

3.1. Market Data

To obtain the market zero-coupon bond term structure, we first build the EUR Euribor-swap curve which is created from the most liquid interest rate instruments available in the market and constructed as follows: We consider deposit rates and Euribor rates with maturity from one day to one year and par-swap rates versus six-month Euribor rates with maturity from two years to thirty years. Then the zero interest curve and the zero-coupon bond curve are calculated using a standard "bootstrapping" technique in conjunction with cubic spline interpolation of the continuously compounded rate (cf. [18] for more details).

We choose two different dates and we take the data at the end of each business day. In particular, we test our model at 30/12/2019 and at 30/11/2020. At the first date, the zero interest rates were negative up to year six, while at the second date the entire zero interest rate structure was negative. In Table 6 and in Table 7 we report the zero interest rate curve and the zero-coupon bond curve at the two different dates.

Furthermore, in Section 3.6 we need the strikes to compute the model swaption prices and the market prices of the swaptions to compare our model, which are for both dates in the Appendix in Table 8, Table 9, Table 10 and Table 11, respectively.

All data has been downloaded from Bloomberg and is used in the following subsections for our numerical experiments. We start in the next subsection with calibrating our model to the zero-coupon curve.

3.2. Calibration

In this subsection we will discuss how we calibrate our model to the market zero-coupon curve given in Table 6 and Table 7 by using the formula derived in (1.5).

Let us denote $\Pi := [\phi_1^x, \phi_2^x, \phi_3^x, \phi_1^y, \phi_2^y, \phi_3^y, x_0, y_0]^T \in \mathbb{R}^8$. We will formulate the calibration procedure as a constraint minimization problem in $\mathbb{R}^8$ for the parameters Π with objective function

$$f(\Pi) := \sum_{i=1}^{n} \left(\frac{P^M(0,T_i)}{P(\Pi;0,T_i)} - 1 \right)^2, \tag{3.1}$$

where $n \in \mathbb{N}$ is the number of time points, where market data is available, and T_i, $i = 1, \dots, n$ are these maturities. The market zero-coupon curve is denoted by $P^M(0,T_i)$ and $P(\Pi;0,T_i)$ is the price of a zero-coupon bond in our model given by (1.5) with parameters Π.

The objective function describes the relative square difference between the market zero-coupon bond prices and the theoretical prices from the model given by (1.5).

The set of admissible parameters $\mathcal{A}$ will consist of the following constraints arising from the well-definedness of the formulas (1.7):

(i) First of all, let us note that there is a one-to-one correspondence between the parameters Π and k_z, σ_z and θ_z if one is looking for positive real solutions only. We have

$$\begin{aligned} k_x &= 2\phi_2^x - \phi_1^x, & k_y &= 2\phi_2^y - \phi_1^y, \\ \sigma_x &= \sqrt{2\left(\phi_2^x\phi_1^x - (\phi_2^x)^2\right)}, & \sigma_y &= \sqrt{-2\left(\phi_2^y\phi_1^y - (\phi_2^y)^2\right)}, \\ \theta_x &= -\frac{\phi_x^2\phi_x^3(\phi_x^1 - \phi_x^2)}{\phi_x^1 - 2\phi_x^2}, & \theta_y &= \frac{\phi_y^2\phi_y^3(\phi_y^1 - \phi_y^2)}{\phi_y^1 - 2\phi_y^2}. \end{aligned} \tag{3.2}$$

(ii) We require $\sigma_z \in \mathbb{R}_{\geq 0}$, $z \in \{x, y\}$. By rearranging (3.2), these conditions are equivalent to $\phi_1^x \geq \phi_2^x$ and $\phi_2^y \geq \phi_1^y$;

(iii) A positive mean-reversion speed, i.e. $k_z \geq 0$, is equivalent to $2\phi_2^z \geq \phi_1^z$, $z \in \{a, b\}$;

(iv) The Feller condition $2k_z\theta_z \geq \sigma_z^2$ is equivalent to $\phi_3^z \geq 1$, $z \in \{a, b\}$;

(v) A positive mean for each CIR process, i.e. $\theta_z \geq 0$, is by positivity of σ_z^2 and k_z equivalent

to $\phi_3^z \geq 0$, which is already satisfied by the Feller condition;

(vi) The parameter ϕ_1^z, assuming that it is real-valued, is positive by definition, meaning that by the positivity of the mean reversion speed, ϕ_2^z will be as well. Therefore, all ϕ are positive;

(vii) As both CIR processes x_t and y_t, individually, are positive processes, we additionally require $x_0 \geq 0$ and $y_0 \geq 0$.

The advantage of using the parameters Π instead of k_z, σ_z and θ_z is that we can rewrite these conditions as a system of linear inequality constraints in matrix notation $A \cdot \Pi \leq 0$, where

$$A := \begin{bmatrix} -1 & 1 & 0 & 0 & 0 & 0 & 0 & 0 \\ 0 & 0 & 0 & 1 & -1 & 0 & 0 & 0 \\ 1 & -2 & 0 & 0 & 0 & 0 & 0 & 0 \\ 0 & 0 & 0 & 1 & -2 & 0 & 0 & 0 \end{bmatrix}$$

with boundary conditions $\Pi_i \geq 0$, $i = 1, \ldots, 8$, and $\Pi_3 = \phi_3^x \geq 1$, as well as $\Pi_6 = \phi_3^y \geq 1$.

In total, the set of admissible parameters is given by

$$\mathcal{A} := \left\{ \Pi \in \mathbb{R}^8_{\geq 0}, \Pi_3, \Pi_6 \geq 1 : A \cdot \Pi \leq 0 \right\}. \tag{3.3}$$

Finally, a solution Π^* to the calibration problem is a minimizer of

$$\min_{\Pi \in \mathcal{A}} f(\Pi). \tag{3.4}$$

To solve (3.4) numerically, we want to use `Matlab`'s function `fmincon` in the (Global) Optimization Toolbox. In order to use this function, we need an initial guess of the parameter Π and the computational time will depend on that choice. In Table 1 we present a few choices for initial guesses of Π. The first row for each date 30/12/2019 or 30/11/2020 refers to `Matlab`'s function `ga` in the (Global) Optimization Toolbox, which uses a generic global optimization algorithm to find a solution of (3.4) without starting from an initial guess, which takes a long time to compute, roughly 35 to 43 seconds. In the following three rows are three manual initial guesses. We can see that the first two choices work for both dates exceptionally fast (0.3 seconds) and the accuracy is almost identical to all other choices, making this model a good choice if live calibration to the data is needed, which we also use in the following numerical experiments. In the last two rows we used random starting parameters to demonstrate that the error remains stable but the computational time varies.

For the algorithms used by `Matlab` we refer the reader to [10], in the context of financial mathematics.

The results of the aforementioned calibration procedure are displayed in Table 2 for both dates 30/12/2019 and 30/11/2020. On the left-hand side, one can see the parameters Π^* and on the right-hand side the corresponding model parameters derived from Π^*. At both dates we obtain good results in fitting the market term structure. The mean relative error (MRE), i.e. $\frac{1}{n}\sum_{i=1}^{n}\left|\frac{P^M(0,T_i)}{P(\Pi^*;0,T_i)} - 1\right|$, over the entire term structure is 0.144 % at the first date and 0.138 % at the second date.

Table 1.: Calibration times and corresponding mean relative errors (MRE) for different initial parameters at 30/12/2019 and 30/11/2020.

Inital Parameter	Times (in s)	MRE (in %)
Calibration at 30/12/2019		
`ga`	42.136	0.142014 %
0.50001 0.50001 1.5 0.50001 0.50001 1.5 0.50001 0.50001	0.287	0.143798 %
1 1 2 1 1 2 1 1	0.229	0.146769 %
1e-05 1e-05 1 1e-05 1e-05 1 1e-05 1e-05	0.276	0.145207 %
0.048808 0.72079 1.4275 0.64469 0.32152 1.4794 0.2556 0.25427	0.334	0.146509 %
0.66073 0.78158 1.5547 0.3779 0.24209 1.249 0.74017 0.63334	103.949	0.14374 %
Calibration at 30/11/2020		
`ga`	35.842	0.135885 %
0.50001 0.50001 1.5 0.50001 0.50001 1.5 0.50001 0.50001	0.280	0.137577 %
1 1 2 1 1 2 1 1	0.188	0.138228 %
1e-05 1e-05 1 1e-05 1e-05 1 1e-05 1e-05	40.864	0.13642 %
0.87647 0.89591 1.4508 0.10496 0.63629 1.3009 0.3297 0.74067	0.185	0.140284 %
0.51541 0.83366 1.9624 0.79757 0.13068 1.6517 0.54064 0.43674	0.342	0.14292 %

Table 2.: Calibration parameters Π^*, model parameters and mean relative errors (MRE) at 30/12/2019 and 30/11/2020, obtained with the market data given in Table 6 and Table 7.

Parameter	30/12/2019	30/11/2020	Parameter	30/12/2019	30/11/2020
ϕ_1^x	0.710501	0.767497	k_x	0.578626	0.631802
ϕ_2^x	0.644564	0.699649	σ_x	0.291551	0.308122
ϕ_3^x	1.60862	1.6014	θ_x	0.118155	0.120319
x_0	0.268914	0.257145			
ϕ_1^y	0.468673	0.523363	k_y	0.59774	0.665895
ϕ_2^y	0.533206	0.594629	σ_y	0.262334	0.291125
ϕ_3^y	1.50249	1.49966	θ_y	0.0864925	0.0954364
y_0	0.280095	0.270007			
$f(\Pi^*)$	$3.247465e-04$	$3.548162e-04$			
MRE	0.144 %	0.138 %			

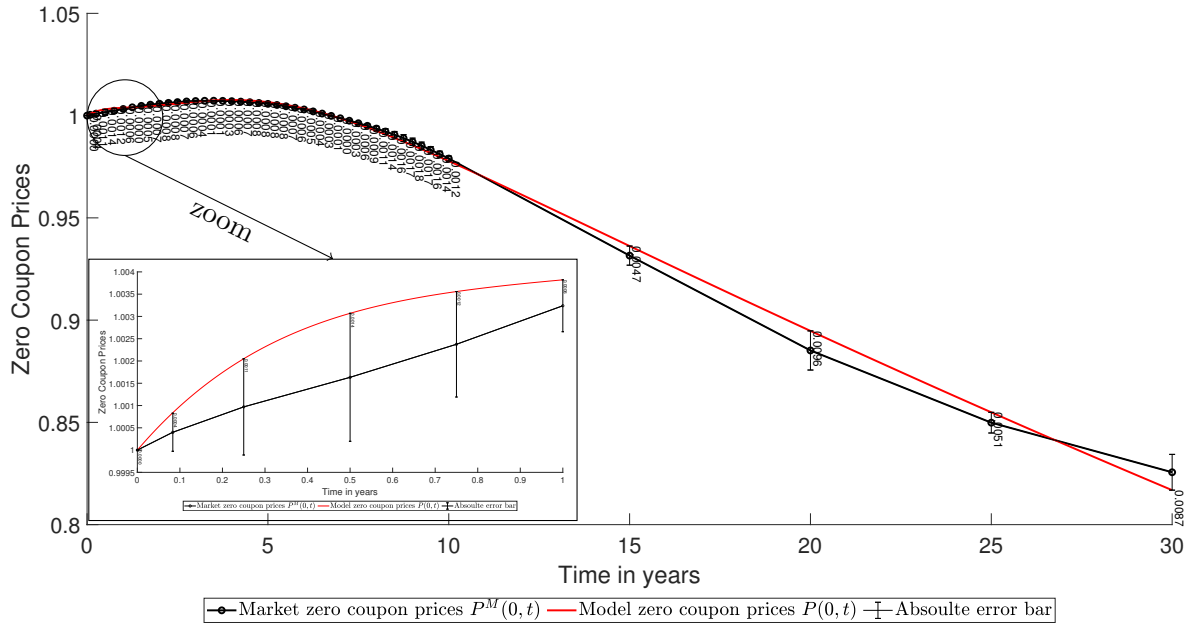

Figure 2.: A comparison of the market zero-coupon prices (Table 6) to the model zero-coupon prices with absolute errors at 30/12/2019 with parameters given in Table 2.

3.3. Euler-Monte-Carlo simulation

In order to forecast the future expected interest rate, we use the Euler-Maruyama scheme to simulate the instantaneous spot rate r (1.3). We refer to [8] and the references therein for a list of different Euler-type methods to simulate a CIR process. In our experiments, we simulate the processes $x(t)$ and $y(t)$ by the truncated Euler scheme defined as follows:

First of all, we fix a homogeneous time grid $0 = t_0 \leq t_1 \leq \cdots \leq t_N = T$ for the interval $[0, T]$ with $N+1$ time points and mesh $\Delta t_i := t_{i+1} - t_i \equiv \Delta := \frac{T}{N}$ for all $i = 0, \ldots, N-1$. Secondly, we simulate the two independent Brownian motions W_z, $z \in \{x, y\}$, and define their time increment as $\Delta W_z(t_i) := W_z(t_{i+1}) - W_z(t_i)$. In total, we compute $r(t_{i+1}) := x(t_{i+1}) - y(t_{i+1})$ for $i = 0, \ldots, N-1$, where

$$\begin{aligned} x(t_{i+1}) &= x(t_i) + k_x(\theta_x - x(t_i))\Delta t_i + \sigma_x \sqrt{\max(x(t_i), 0)} \Delta W_x(t_i) \\ y(t_{i+1}) &= y(t_i) + k_y(\theta_y - y(t_i))\Delta t_i + \sigma_y \sqrt{\max(y(t_i), 0)} \Delta W_y(t_i). \end{aligned} \tag{3.5}$$

We choose the max inside the square-root to ensure that the square-root remains real, because due to discretization effects the positivity of $x(t_i)$ and $y(t_i)$ might be violated.

In the following experiments we choose $\Delta = \frac{1}{256}$ and use $M = 10000$ samples for each of the Brownian motions. In Figure 3 we show the mean and 99.9 % confidence interval (under the assumption of the central limit theorem) of the model discount factors compared to the market discount factors at 30/12/2019. One can see that the mean does not differ from the market discount factors very much till 5 years with an error of magnitude 0.005 and increases slightly to a magnitude of 0.05 afterwards till 30 years.

A more detailed comparison of the mean absolute errors, i.e. the absolute value of the

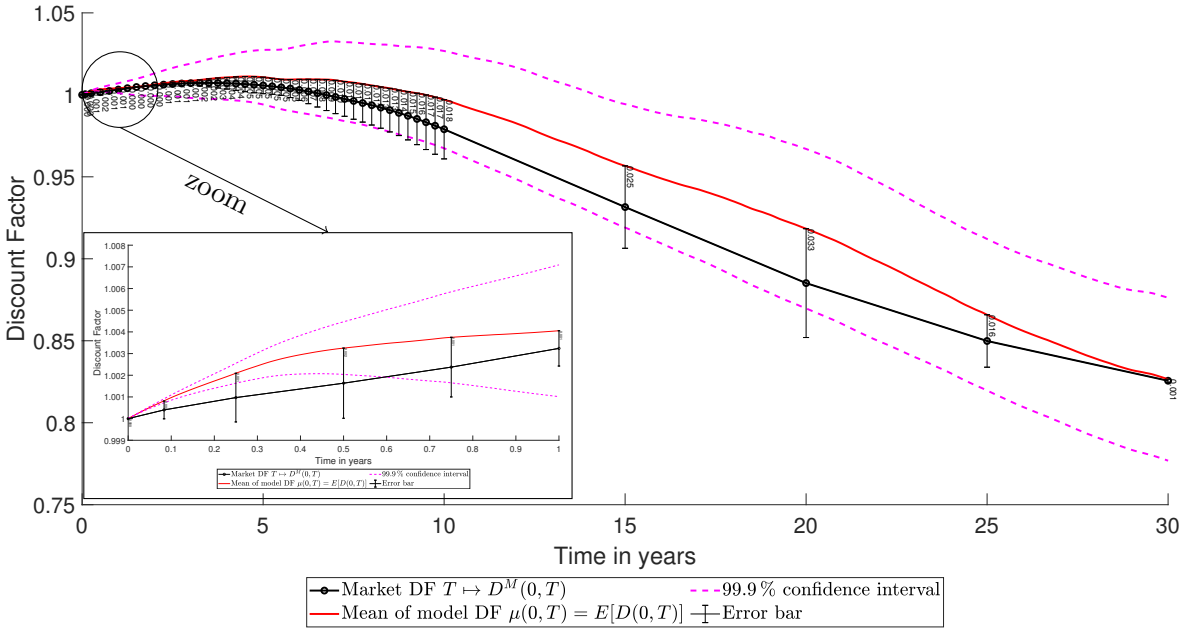

Figure 3.: A comparison of the market discount factors (Table 6) to the mean of the model discount factors with absolute errors at 30/12/2019 with parameters given in Table 2 by using (3.5) with $\Delta = \frac{1}{256}$ and $M = 10000$.

difference of the mean over all simulations of our model to the market data, at each maturity can be found in the appendix in Table 5.

3.4. Mean and variance

The $\mathcal{F}_s$-conditional mean and variance of the CIR process are well-known (cf. [5] p. 66 equation (3.23)) and are given by

$$E_s^{\mathbb{Q}}[z(t)] = z(s)e^{-k_z(t-s)} + \theta_z\left(1 - e^{-k_z(t-s)}\right)$$
$$\mathrm{Var}_s^{\mathbb{Q}}[z(t)] = z(s)\frac{\sigma_z^2}{k_z}\left(e^{-k_z(t-s)} - e^{-2k_z(t-s)}\right) + \theta_z\frac{\sigma_z^2}{2k_z}\left(1 - e^{-k_z(t-s)}\right)^2,$$

where $z \in \{x, y\}$. In the case of the difference of two CIR processes we have

$$E_s^{\mathbb{Q}}[r(t)] = E_s^{\mathbb{Q}}[x(t) - y(t)] = E_s^{\mathbb{Q}}[x(t)] - E_s^{\mathbb{Q}}[y(t)] \tag{3.6}$$

and by independence

$$\mathrm{Var}_s^{\mathbb{Q}}[r(t)] = \mathrm{Var}_s^{\mathbb{Q}}[x(t)] + \mathrm{Var}_s^{\mathbb{Q}}[y(t)]\,. \tag{3.7}$$

In Figure 5 we show for each date the histogram of the short rate distribution after 30 years. To describe the distribution of $r(t)$ after 30 years better, we also compare it to the density of a normal random variable with the same mean and variance. As one expects, the distribution of r shows a slight skewness and fatter tail with respect to the normal distribution.

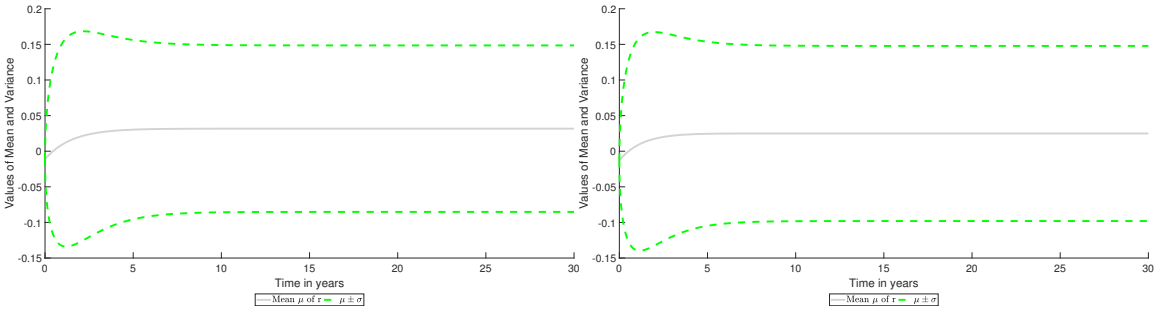

Figure 4.: Mean and standard deviation of $r(t)$ using the calibrated parameters in Table 2, obtained with (3.6) and (3.7). The left picture shows the results at 30/12/2019 and the right at 30/11/2020.

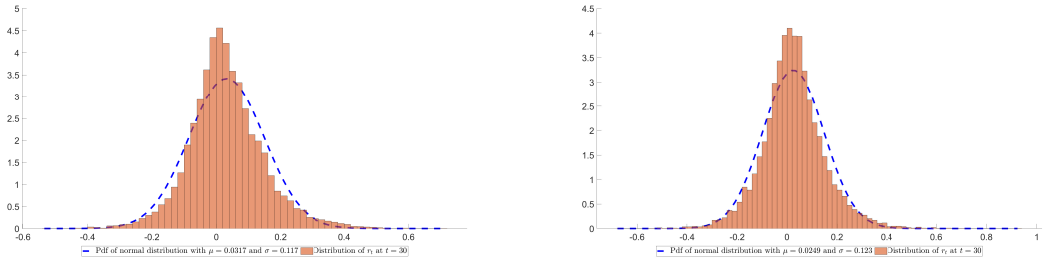

Figure 5.: Distribution of the simulated short rate $r(t)$ compared to the normal distribution at $t = 30$ using the calibrated parameters in Table 2, $\Delta = \frac{1}{256}$ and $M = 10000$. The left picture shows the results at 30/12/2019 and the right at 30/11/2020.

3.5. t-Forward zero-coupon prices

In this subsection we examine, if our model is able to replicate the interest rate term structure not only at the start date but also in the future. Therefore, we compare the market and model prices of zero-coupon bonds at future times t by using the continuously-compounded spot interest rates (cf. [5] Definition 1.2.3.) to obtain the market prices.

To be more precise, let us briefly recall the definition of the continuously-compounded spot interest rates

$$R(t,T) := -\frac{\log P(t,T)}{T-t}, \tag{3.8}$$

where we use the day-count convention $T - t$ in years.

To compute this rate for the market at a fixed future date $t > 0$ with maturity $T > t$ we use

$$R^M(t,T) := \frac{TR^M(0,T) - tR^M(0,t)}{T-t} \tag{3.9}$$

where $R^M(0,t)$ and $R^M(0,T)$ are the market zero rates with maturity t and T respectively.

By rearranging (3.8) we derive the market zero-coupon price at a future date t with maturity T as

$$P^M(t,T) = \exp\left(-R^M(t,T)(T-t)\right). \tag{3.10}$$

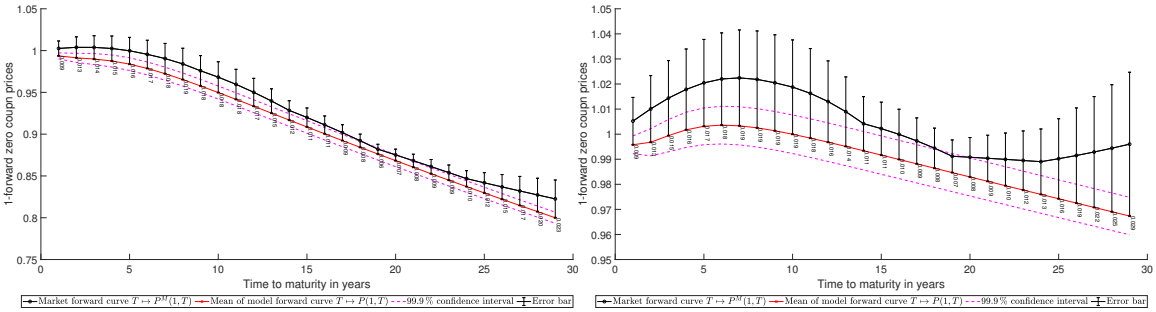

Figure 6.: Mean and 99 % confidence interval of the model t-forward zero-coupon prices compared to the market t-forward zero-coupon prices at $t = 1$ using the calibrated parameters in Table 2, $\Delta = \frac{1}{256}$ and $M = 10000$. The left picture shows the results at 30/12/2019 and the right at 30/11/2020.

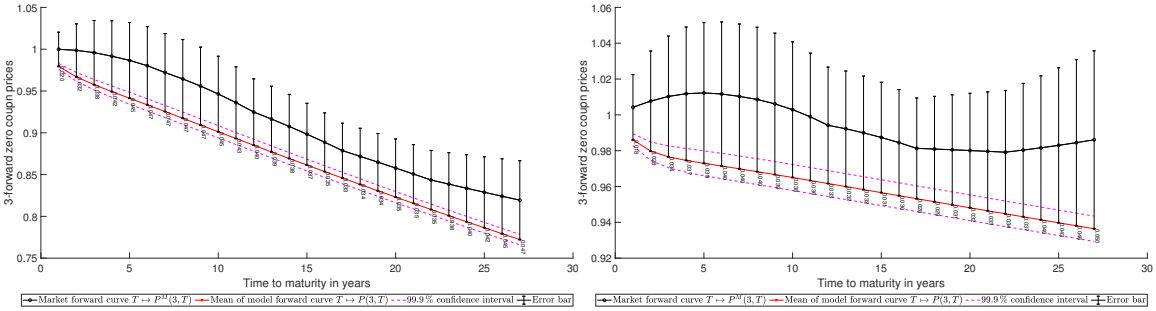

Figure 7.: Mean and 99 % confidence interval of the model t-forward zero-coupon prices compared to the market t-forward zero-coupon prices at $t = 3$ using the calibrated parameters in Table 2, $\Delta = \frac{1}{256}$ and $M = 10000$. The left picture shows the results at 30/12/2019 and the right at 30/11/2020.

Now, we can compare (3.10) to the mean over all simulated trajectories of the model t-forward zero-coupon price derived from (1.5).

In Figure 6, Figure 7 and Figure 8 we show a comparison of (3.10) to (1.5) at 30/12/2019 and 30/11/2020 with parameters Π^* from Table 2 for future times $t = 1, 3, 5$, respectively.

The behavior shown by the model t-forward prices coincides with typical one-factor short interest rate models. At short future dates, one year for example, the model is able to reproduce the market forward zero-coupon price for 30/12/2019, i.e. the error is of magnitude 0.01, whereas at long future dates, e.g. Figure 8, the model prices are deviating further from the market prices, i.e. the error is of magnitude 0.03. For 30/11/2020 we can see that the errors are not very large but the model seems to have difficulties to match the shape of the predicted market prices.

3.6. Pricing swaptions

In this subsection we test if our model is market consistent, in the sense whether the model is able to reproduce market swaption prices or not.

We compare market swaption prices to model swaption prices with different tenors $(1, 2, 5, 7, 10$ years) and maturities $(1, 2, 5, 7, 10, 15, 20$ years). The market swaption prices are computed by Bachelier's formula from normal volatilities quoted in the market whereas the model swap-

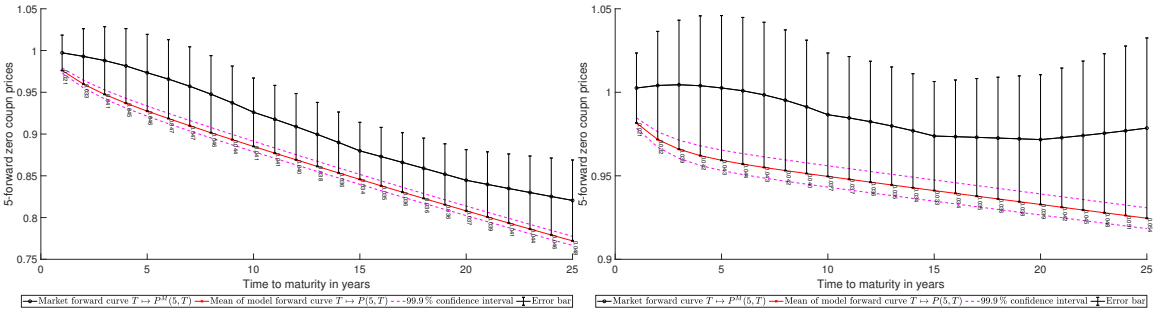

Figure 8.: Mean and 99 % confidence interval of the model t-forward zero-coupon prices compared to the market t-forward zero-coupon prices at $t = 5$ using the calibrated parameters in Table 2, $\Delta = \frac{1}{256}$ and $M = 10000$. The left picture shows the results at 30/12/2019 and the right at 30/11/2020.

Table 3.: 30/12/2019: difference between swaption model price and swaption market price

Maturity \ Tenor	1	2	5	7	10
1	4.82602 %	3.72741 %	1.56009 %	0.601718 %	−0.554628 %
2	4.70047 %	3.56775 %	1.18057 %	0.0467543 %	−1.37405 %
5	3.60511 %	2.4125 %	−0.249531 %	−1.64559 %	−3.50471 %
7	3.23362 %	1.97696 %	−0.945175 %	−2.48803 %	−4.54551 %
10	2.85895 %	1.49467 %	−1.69265 %	−3.37829 %	−5.63478 %
15	2.63259 %	1.17927 %	−2.21714 %	−4.05043 %	−6.53224 %
20	2.48029 %	1.01554 %	−2.47166 %	−4.39298 %	−6.98019 %

tion prices are from the simulated future zero-coupon prices in (1.5). The difference between market price to model prices for 30/12/2019 and 30/11/2020 are reported in Table 3 and Table 4, respectively. We notice that, similar to one-factor short interest rate model, our model fails to capture the full swaption volatility surface. This result is not surprising, since the model uses essentially a single volatility factor due to the fact that the model parameters are constant and the Brownian motion are independent. A way to make the model able to match the entire volatility surface is the inclusion of time-dependent parameters to fit exactly the market term structure or, equivalently, adding a deterministic function of time to the short rate process r, which is left for future research.

Table 4.: 30/11/2020: difference between swaption model price and swaption market price

Maturity \ Tenor	1	2	5	7	10
1	4.87829 %	3.71571 %	1.62322 %	0.745822 %	−0.307305 %
2	4.62191 %	3.4627 %	1.22337 %	0.167669 %	−1.18931 %
5	3.82762 %	2.596 %	−0.0624237 %	−1.4526 %	−3.34358 %
7	3.45837 %	2.13705 %	−0.80375 %	−2.35496 %	−4.46368 %
10	3.24577 %	1.77121 %	−1.56541 %	−3.3177 %	−5.74088 %
15	3.02788 %	1.4328 %	−2.26341 %	−4.2787 %	−7.03714 %
20	3.16548 %	1.42331 %	−2.6344 %	−4.8421 %	−7.85129 %

4. Conclusion and future research

In this paper, we propose a new model to handle the challenges arising from negative interest rates, while preserving the analytical tractability of the original CIR model without introducing any shift to the market interest rates. The strength of our model is that it is very simple, fast to calibrate and fits the present market term structure very well for an essentially one-factor short rate model.

Let us briefly summarize our discoveries of the numerical section. We show that the distribution of the short rate after 30 years has similar features compared to the original CIR model in terms of skewness and fat tail. At 30/12/2019 we show that the model is quite capable of pricing zero-bonds at future times, while for 30/11/2020 the error is not too large but an improvement of the current model would be desirous to allow a better fit to the shape of the market prices. Similarly, we show that we require an extension of the model to price swaptions more accurately.

That being said, the authors would like to stress that this is a first step in this methodology of using two CIR processes as a difference to model negative interest rates. Naturally, its extensions, such as considering time-dependent coefficients to fit the market term structure perfectly or, equivalently, adding a deterministic shift extension in the sense of [5], will be a next step and is left for future research.

A. Derivation of the Riccati equations and coefficients

Let everything be as in Lemma 2.1. In particular, let

$$P(t,T) \stackrel{!}{=} A_x(t,T)\exp\left(-B_x(t,T)x(t)\right)A_y(t,T)\exp\left(B_y(t,T)y(t)\right).$$

To derive the Riccati equations (2.3) we use the fact, that we are modelling under the martingale measure $\mathbb{Q}$, therefore the discounted price process $\exp\left(-\int_0^t r(s)ds\right)P(t,T)$ needs to be a martingale.

By independence of x and y, as well as Itô's formula we derive after some algebra

$$
\begin{aligned}
&d\left[\exp\left(-\int_0^t r(s)ds\right) A_x(t,T)\exp\left(-B_x(t,T)x(t)\right) A_y(t,T)\exp\left(B_y(t,T)y(t)\right)\right] \\
&\quad = A_x(t,T)\exp\left(-\int_0^t x(s)ds - B_x(t,T)x(t)\right)\Bigg[\exp\left(\int_0^t y(s)ds + B_y(t,T)y(t)\right)\Bigg[\\
&\qquad A_y(t,T)\Big[y(t)dt + B_y(t,T)dy(t) + y(t)\left(\partial_t B_y\right)(t,T)dt + \frac{1}{2}B_y^2(t,T)d\left\langle y\right\rangle_t\Big] \\
&\qquad + \left(\partial_t A_y\right)(t,T)dt\Bigg]\Bigg] \\
&\quad + A_y(t,T)\exp\left(\int_0^t y(s)ds + B_y(t,T)y(t)\right)\Bigg[\exp\left(-\int_0^t x(s)ds + B_x(t,T)x(t)\right)\Bigg[\\
&\qquad A_x(t,T)\Big[-x(t)dt - B_x(t,T)dx(t) - x(t)\left(\partial_t B_x\right)(t,T)dt + \frac{1}{2}B_x^2(t,T)d\left\langle x\right\rangle_t\Big] \\
&\qquad + \left(\partial_t A_x\right)(t,T)dt\Bigg]\Bigg].
\end{aligned}
$$

Now, in order to be a martingale the parts of bounded variation have to vanish, which leads us after rearranging the terms to

$$
\begin{aligned}
0 \overset{!}{=}\ & y(t)\Big[A_x(t,T)A_y(t,T)\Big[1 + B_y(t,T)\lambda_y(t) + \left(\partial_t B_y\right)(t,T) + \frac{1}{2}B_y^2(t,T)\gamma_y(t)\Big]\Big] \\
&+ x(t)\Big[A_y(t,T)A_x(t,T)\Big[-1 - B_x(t,T)\lambda_x(t) - \left(\partial_t B_x\right)(t,T) + \frac{1}{2}B_x^2(t,T)\gamma_x(t)\Big]\Big] \\
&+ A_x(t,T)A_y(t,T)\Big[B_y(t,T)\eta_y(t) + \frac{1}{2}B_y^2(t,T)\delta_y(t) - B_x(t,T)\eta_x(t) + \frac{1}{2}B_x^2(t,T)\delta_x(t)\Big] \\
&+ A_x(t,T)\left(\partial_t A_y\right)(t,T) + A_y(t,T)\left(\partial_t A_x\right)(t,T).
\end{aligned}
$$

Thus, we derive the following Riccati System

$$
\begin{aligned}
1 + B_y(t,T)\lambda_y(t) + \left(\partial_t B_y\right)(t,T) + \frac{1}{2}B_y^2(t,T)\gamma_y(t) = 0, &\qquad B_y(T,T) = 0, \\
-1 - B_x(t,T)\lambda_x(t) - \left(\partial_t B_x\right)(t,T) + \frac{1}{2}B_x^2(t,T)\gamma_x(t) = 0, &\qquad B_x(T,T) = 0, \\
B_y(t,T)\eta_y(t) + \frac{1}{2}B_y^2(t,T)\delta_y(t) - B_x(t,T)\eta_x(t) + \frac{1}{2}B_x^2(t,T)\delta_x(t) & \\
+ \partial_t\left(\log A_y\right)(t,T) + \partial_t\left(\log A_x\right)(t,T) = 0. &
\end{aligned}
$$

A solution to the last equation can be found by further assuming that the individual x and y parts will be zero, leading to two separate equations

$$
\begin{aligned}
B_y(t,T)\eta_y(t) + \frac{1}{2}B_y^2(t,T)\delta_y(t) + \partial_t\left(\log A_y\right)(t,T) = 0, &\quad A_y(T,T) = 1, \\
-B_x(t,T)\eta_x(t) + \frac{1}{2}B_x^2(t,T)\delta_x(t) + \partial_t\left(\log A_x\right)(t,T) = 0, &\quad A_x(T,T) = 1.
\end{aligned}
$$

We will now turn to the special case of the CIR processes (1.4). We see immediately that the equations for x are in the usual form and defining $\lambda_x(t) \equiv -k_x, \eta_x(t) \equiv k_x\theta_x, \gamma_x(t) \equiv \sigma_x^2, \delta_x(t) \equiv 0$ yields the explicit solution from the literature (cf. [5] p. 66 equation (3.25)).

Concerning the y terms, we make the following educated guess and verify, that it solves the equation:

$$\begin{aligned} A(t,T) &= \left(\frac{2h\exp\left((k+h)(T-t)/2\right)}{2h+(k+h)\left(\exp\left((T-t)h\right)-1\right)},\right)^{\frac{2k\theta}{\sigma^2}} \\ B(t,T) &= \frac{2\left(\exp\left((T-t)h\right)-1\right)}{2h+(k+h)\left(\exp\left((T-t)h\right)-1\right)}, \\ h &= \sqrt{k^2-2\sigma^2}, \end{aligned}$$

where we will drop the index for indicating that we are considering the y coefficients for readability and assume that $k^2 \geq 2\sigma^2$.

Verification for B We will first check the formula for the Riccati equation in B:

We will now simplify the nominator and the denominator of $\partial_t B + \frac{1}{2}\sigma^2 B^2 - kB$, which is given by

$$\begin{aligned} &\partial_t B + \frac{1}{2}\sigma^2 B^2 - kB = \\ &\frac{\sigma^2\left(2\,\mathrm{e}^{\sqrt{k^2-2\,\sigma^2}\,(T-t)}-2\right)^2}{2\left(\left(\mathrm{e}^{\sqrt{k^2-2\,\sigma^2}\,(T-t)}-1\right)\left(k+\sqrt{k^2-2\,\sigma^2}\right)+2\sqrt{k^2-2\,\sigma^2}\right)^2} \\ &-\frac{2\,\mathrm{e}^{\sqrt{k^2-2\,\sigma^2}\,(T-t)}\sqrt{k^2-2\,\sigma^2}}{\left(\mathrm{e}^{\sqrt{k^2-2\,\sigma^2}\,(T-t)}-1\right)\left(k+\sqrt{k^2-2\,\sigma^2}\right)+2\sqrt{k^2-2\,\sigma^2}} \\ &-\frac{k\left(2\,\mathrm{e}^{\sqrt{k^2-2\,\sigma^2}\,(T-t)}-2\right)}{\left(\mathrm{e}^{\sqrt{k^2-2\,\sigma^2}\,(T-t)}-1\right)\left(k+\sqrt{k^2-2\,\sigma^2}\right)+2\sqrt{k^2-2\,\sigma^2}} \\ &+\frac{\mathrm{e}^{\sqrt{k^2-2\,\sigma^2}\,(T-t)}\sqrt{k^2-2\,\sigma^2}\left(k+\sqrt{k^2-2\,\sigma^2}\right)\left(2\,\mathrm{e}^{\sqrt{k^2-2\,\sigma^2}\,(T-t)}-2\right)}{\left(\left(\mathrm{e}^{\sqrt{k^2-2\,\sigma^2}\,(T-t)}-1\right)\left(k+\sqrt{k^2-2\,\sigma^2}\right)+2\sqrt{k^2-2\,\sigma^2}\right)^2}. \end{aligned}$$

After bringing the terms to the common denominator, we consider now the nominator of this transformation

$$\begin{aligned} &\frac{1}{2}\sigma^2\left(2\exp\left(\sqrt{k^2-2\sigma^2}\tau\right)-2\right)^2 \\ &\quad-\left(2\sqrt{k^2-2\sigma^2}\exp\left(\sqrt{k^2-2\sigma^2}\tau\right)+k\left(2\exp\left(\sqrt{k^2-2\sigma^2}\tau\right)-2\right)\right) \\ &\qquad\left(\left(\exp\left(\sqrt{k^2-2\sigma^2}\tau\right)-1\right)\left(k+\sqrt{k^2-2\sigma^2}\right)+2\sqrt{k^2-2\sigma^2}\right) \\ &\quad+\exp\left(\sqrt{k^2-2\sigma^2}\tau\right)\sqrt{k^2-2\sigma^2}\left(k+\sqrt{k^2-2\sigma^2}\right)\left(2\exp\left(\sqrt{k^2-2\sigma^2}\tau\right)-2\right) \\ &=2\,h\,k-2\,k^2-2\,k^2\,\mathrm{e}^{2\,h\,\tau}+2\,\sigma^2+4\,\sigma^2\,\mathrm{e}^{h\,\tau}+2\,\sigma^2\,\mathrm{e}^{2\,h\,\tau}-2\,h\,k\,\mathrm{e}^{2\,h\,\tau}, \end{aligned}$$

where we substituted $\tau := T-t$ and $h := \sqrt{k^2-2\sigma^2}$. The denominator can be simplified in

the same way, leading to

$$2\,k^2 - 2\,h\,k + 2\,k^2\,\mathrm{e}^{2\,h\,\tau} - 2\,\sigma^2 - 4\,\sigma^2\,\mathrm{e}^{h\,\tau} - 2\,\sigma^2\,\mathrm{e}^{2\,h\,\tau} + 2\,h\,k\,\mathrm{e}^{2\,h\,\tau}.$$

In total, we see that the denominator differs only by a sign, hence $\partial_t B + \frac{1}{2}\sigma^2 B^2 - kB = -1$, which yields the claim.

Verification for A The formula can be derived by just integrating and taking the exponential.

$$\left(\frac{2h\mathrm{e}^{\frac{1}{2}\tau(k+h)}}{(\mathrm{e}^{\tau\,h}-1)\,(h+k)+2h}\right)^{\frac{2\,k\,\theta}{\sigma^2}},$$

where $h \coloneqq \sqrt{k^2 - 2\,\sigma^2}$ and $\tau \coloneqq T - t$.

Let us just take the logarithm and derivative to verify this formula:

$$\log\left(A(\tau)\right) = \frac{\tau\,\left(2\,k^2\,\theta + 2\,k\,\theta\,h\right)}{2\,\sigma^2} - \frac{2\,k\,\theta\,\ln\left(\mathrm{e}^{\tau\,h}\,h - k + h + k\,\mathrm{e}^{\tau\,h}\right)}{\sigma^2} + \frac{2\,k\,\theta\,\ln\left(2\,\sqrt{k^2 - 2\,\sigma^2}\right)}{\sigma^2}.$$

Now, taking the derivative yields

$$\partial_\tau\left(\log\left(A\left(\tau\right)\right)\right) = \frac{2\,k\,\theta\,\left(\mathrm{e}^{\tau\,h}-1\right)}{\mathrm{e}^{\tau\,h}\,h - k + h + k\,\mathrm{e}^{\tau\,h}} = k\theta\frac{2\left(\mathrm{e}^{\tau\,h}-1\right)}{(\mathrm{e}^{\tau\,h}-1)\,(h+k)+2h}.$$

After undoing the substitution for τ this is equal to $k\theta B$, which yields the claim.

B. Instantaneous forward rate

The definition of the instantaneous forward rate (cf. [5] p. 13 equation (1.23)) is given by

$$f(t,T) \coloneqq -\partial_T \log\left(P\left(t,T\right)\right).$$

By (1.5) we therefore have

$$\begin{aligned}
f(t,T) &= -\partial_T\left(\log\left(A_x(t,T)e^{-B_x(t,T)x(t)}A_y(t,T)e^{B_y(t,T)y(t)}\right)\right)\\
&= -\partial_T\left(\log\left(A_x(t,T)\right) - B_x(t,T)x(t)\right) - \partial_T\left(\log\left(A_y(t,T)\right) + B_y(t,T)y(t)\right)\\
&= -\frac{\partial_T\left(A_x(t,T)\right)}{A_x(t,T)} + \partial_T\left(B_x(t,T)\right)x(t) - \frac{\partial_T\left(A_y(t,T)\right)}{A_y(t,T)} - \partial_T\left(B_y(t,T)\right)y(t).
\end{aligned}$$

Let $z \in \{x, y\}$ and consider the case of the CIR model (1.4). Then those derivatives are given by the following expressions: Let us calculate the derivative of A_z first

$$\begin{aligned}&\partial_T \left(A_z(t,T)\right)\\ &= \phi_z^3 \left(\frac{\phi_z^1 \phi_z^2 e^{\phi_z^2 (T-t)}}{\phi_z^1 + \phi_z^2 \left(e^{\phi_z^1 (T-t)} - 1\right)} - \frac{\left(\phi_z^1\right)^2 \phi_z^2 e^{\phi_z^1 (T-t)} e^{\phi_z^2 (T-t)}}{\left(\phi_z^1 + \phi_z^2 \left(e^{\phi_z^1 (T-t)} - 1\right)\right)^2} \right) \left(\frac{\phi_z^1 e^{\phi_z^2 (T-t)}}{\phi_z^1 + \phi_z^2 \left(e^{\phi_z^1 (T-t)} - 1\right)} \right)^{\phi_z^3 - 1}.\end{aligned}$$

Hence, we get

$$-\frac{\partial_T \left(A_x(t,T)\right)}{A_x(t,T)} = \frac{\phi_z^2 \phi_z^3 \left(\phi_z^1 - \phi_z^2\right) \left(e^{(T-t)\phi_z^1} - 1\right)}{\phi_z^1 + \phi_z^2 \left(e^{(T-t)\phi_z^1} - 1\right)}.$$

Now, we compute the derivative of B_z

$$\partial_T \left(B_z(t,T)\right) = \frac{\left(\phi_z^1\right)^2 e^{(T-t)\phi_z^1}}{\left(\phi_z^1 + \phi_z^2 \left(e^{(T-t)\phi_z^1} - 1\right)\right)^2}.$$

C. Mean error of discount factors

Table 5.: Mean error of discount factors (DF) of our model with parameters given in Table 2 at 30/12/2019 and 30/11/2020.

Maturity (in years)	Mean Error of DF at 30/12/2019	Mean Error of DF at 30/11/2020
0.0833333	0.000409963	0.000560815
0.25	0.00112268	0.00119113
0.5	0.00161849	0.00144972
0.75	0.00137477	0.00113393
1	0.000814101	0.000550498
1.25	0.000328491	0.000398677
1.5	$1.4362e-05$	0.000571146
1.75	$5.62967e-05$	0.000805009
2	0.000402274	0.00125292
2.25	0.000824884	0.00191315
2.5	0.0011063	0.00288173
2.75	0.00133005	0.00356734
3	0.00143482	0.00401817
3.25	0.0018223	0.00441028
3.5	0.00242705	0.00477583
3.75	0.00303645	0.00512345
4	0.00354305	0.00537247
4.25	0.00409665	0.0051572
4.5	0.00461513	0.00473785
4.75	0.00491301	0.00449665
5	0.00502117	0.00423046
5.25	0.00485501	0.00398605
5.5	0.0048752	0.00410309
5.75	0.00549422	0.00442951
6	0.00642713	0.00477755
6.25	0.00743045	0.00495872
6.5	0.00841358	0.00514248
6.75	0.00945159	0.00546137
7	0.010154	0.00596334
7.25	0.0105884	0.006623
7.5	0.0111652	0.00753078
7.75	0.0116295	0.00803137
8	0.0120698	0.00842589
8.25	0.0125788	0.00889094
8.5	0.0132799	0.00938679
8.75	0.0138392	0.00983092
9	0.0146873	0.0100521
9.25	0.0156794	0.0103367
9.5	0.0166502	0.0109601
9.75	0.0174248	0.0117957
10	0.0180652	0.0126498
15	0.0251373	0.0314676
20	0.0331911	0.0233781
25	0.0160001	0.0174282
30	0.00094742	0.00846645

D. Market data

Table 6.: Market data containing the zero rate curve and zero coupon curve at 30/12/2019.

Maturity (in years)	Zero rate (in %)	Zero-coupon price
0.0833333333333333	−0.469999993219972	1.0004001991529
0.25	−0.388000020757318	1.00096969387991
0.5	−0.324999983422458	1.00163343819125
0.75	−0.314333918504417	1.00237481461989
1	−0.322000007145107	1.00323926670136
1.25	−0.323286440253412	1.00405360258242
1.5	−0.316161320131414	1.00476558980205
1.75	−0.303842297803669	1.00535001652119
2	−0.289547047577798	1.00582418019158
2.25	−0.275860329135469	1.00623288634409
2.5	−0.262835313503729	1.006604855007
2.75	−0.249892233800608	1.00691299093433
3	−0.236451346427202	1.00713375064174
3.25	−0.222084053437044	1.00725039326453
3.5	−0.20696636298112	1.00728054250496
3.75	−0.191425434683623	1.00721781901104
4	−0.175788428168744	1.00706740209126
4.25	−0.160311330630236	1.00684531811395
4.5	−0.144965462482105	1.00655553463348
4.75	−0.129650957156002	1.00618948972951
5	−0.114267959725112	1.00573933685071
5.25	−0.0987154224631581	1.00520062530541
5.5	−0.0828875612342017	1.00457454544122
5.75	−0.0666773874613114	1.00384671986489
6	−0.0499779242090881	1.00300667524933
6.25	−0.0327643402378897	1.00205088034181
6.5	−0.0153403983915723	1.00099833086134
6.75	0.00190798987986796	0.999871102605028
7	0.0185949131264351	0.998698306220564
7.25	0.0344518735623467	0.997505079039002
7.5	0.0496800311054812	0.996279818846146
7.75	0.0645979575189415	0.995003816465917
8	0.0795242260210216	0.993656440330286
8.25	0.0947347900819295	0.992214008696662
8.5	0.110335148849572	0.990662992494919
8.75	0.126388167535652	0.988997743889118
9	0.142956722993404	0.987213788328959
9.25	0.160050573928316	0.985308478446392
9.5	0.177466994199449	0.983284710270437
9.75	0.194950156980411	0.981173005874126
10	0.212244223803282	0.979004189945635
15	0.473523046821356	0.931543316237289
20	0.611338950693607	0.885166902653398
25	0.652327481657267	0.849865688031976
30	0.640345783904195	0.825611308910539

Table 7.: Market data containing the zero rate curve and zero coupon curve at 30/11/2020.

Maturity (in years)	Zero rate (in %)	Zero-coupon price
0.0833333333333333	−0.499999988824129	1.00041207460911
0.244444444444444	−0.526142632588744	1.00130160930003
0.5	−0.507755391299725	1.00252751322004
0.75	−0.503638433292508	1.00378359716281
1	−0.517199980095029	1.00519888845098
1.24444444444444	−0.524928161568994	1.00658242962185
1.5	−0.525975602238304	1.00791998180754
1.75	−0.522984338103072	1.00920759910672
2	−0.518596358597279	1.01045317135578
2.24444444444444	−0.514924664329897	1.01166557509739
2.5	−0.511966253088758	1.0128933501334
2.75	−0.509189122195153	1.01412683679008
3	−0.50606126897037	1.01533680279481
3.24722222222222	−0.502153361016866	1.0164921683478
3.5	−0.497446840398652	1.01760034898714
3.75	−0.492025761253245	1.01867206863544
4	−0.485974224284291	1.01969106459461
4.24444444444444	−0.479376664922526	1.02062910472473
4.5	−0.47231881015648	1.02152663951854
4.75	−0.464886791550967	1.02238363928715
5	−0.457166694104671	1.02318805666289
5.24444444444444	−0.449221897941854	1.02391569856637
5.5	−0.441024916645461	1.0246017102629
5.75	−0.432525547282481	1.02524040701367
6	−0.423673586919904	1.02581359580938
6.24444444444444	−0.414435069675712	1.02629288605375
6.5	−0.404840884313273	1.02671307570551
6.75	−0.394938214854612	1.02707383363012
7	−0.384774198755622	1.02736441987847
7.24722222222222	−0.37439006592308	1.02757527517123
7.5	−0.363803462582268	1.02771717281163
7.75	−0.353026057560157	1.0277994267812
8	−0.342069566249847	1.02781095336332
8.24444444444444	−0.330958580803831	1.02773379298185
8.5	−0.319769247063562	1.02760240180053
8.75	−0.308590599271419	1.02742329257773
9	−0.297511671669781	1.02719551414522
9.24444444444444	−0.286599750659389	1.02691014728746
9.5	−0.275835084599585	1.02659173861864
9.75	−0.265176203111905	1.02623638422587
10	−0.254581612534821	1.02583261454546
15	−0.0622837862465531	1.00939445284171
20	0.0184025324415416	0.996324084241296
25	0.0234601888223551	0.994148968990786
30	−0.00393075206375215	1.00118069913068

Table 8.: Market data containing the swaption prices at 30/12/2019.

Maturity \ Tenor	1	2	5	7	10
1	0.000702236	0.00175071	0.00706456	0.0112631	0.0181169
2	0.0014433	0.00333027	0.0111956	0.017189	0.0265694
5	0.00391314	0.00796766	0.0214221	0.0308074	0.0453508
7	0.00521117	0.0104082	0.0268942	0.0380283	0.0548627
10	0.00668368	0.0132567	0.0330802	0.045932	0.0651091
15	0.00781681	0.0154396	0.0378811	0.0525334	0.0743464
20	0.00840243	0.0166069	0.0407885	0.0565876	0.0795953

Table 9.: Market data containing the swaption prices at 30/11/2020.

Maturity \ Tenor	1	2	5	7	10
1	0.000661505	0.00151259	0.00547626	0.00900521	0.0149394
2	0.00121578	0.00278226	0.00916199	0.0145571	0.0235389
5	0.00336776	0.00707345	0.0194074	0.0285692	0.0433793
7	0.0047279	0.00963075	0.0253482	0.0364087	0.0537919
10	0.00630168	0.0126162	0.0323949	0.0456958	0.0665005
15	0.00790807	0.0157371	0.0397201	0.0558865	0.0802858
20	0.00898181	0.017927	0.0451252	0.0631302	0.0898938

Table 10.: Market data containing the swaption strikes at 30/12/2019.

Maturity \ Tenor	1	2	5	7	10
1	−0.260793 %	−0.195187 %	−0.011405 %	0.140129 %	0.330514 %
2	−0.129665 %	−0.0782444 %	0.139932 %	0.273273 %	0.449172 %
5	0.268095 %	0.38307 %	0.556996 %	0.655339 %	0.757978 %
7	0.547079 %	0.611571 %	0.76683 %	0.830788 %	0.891069 %
10	0.880582 %	0.907944 %	0.967521 %	0.988131 %	0.992003 %
15	1.04232 %	1.04153 %	1.01776 %	0.985317 %	0.924744 %
20	0.925377 %	0.901441 %	0.827386 %	0.778437 %	0.721445 %

Table 11.: Market data containing the swaption strikes at 30/11/2020.

Maturity \ Tenor	1	2	5	7	10
1	−0.558066 %	−0.544838 %	−0.455765 %	−0.37221 %	−0.238803 %
2	−0.531679 %	−0.502856 %	−0.386908 %	−0.294521 %	−0.162606 %
5	−0.315638 %	−0.264729 %	−0.117094 %	−0.0324645 %	0.0536401 %
7	−0.117189 %	−0.0652544 %	0.0603589 %	0.1157 %	0.150538 %
10	0.150213 %	0.179568 %	0.225372 %	0.223805 %	0.196761 %
15	0.234862 %	0.219855 %	0.16784 %	0.12791 %	0.0641018 %
20	0.0500327 %	0.0277677 %	−0.0398808 %	−0.0837531 %	−0.134806 %

Declarations

Funding

This project has received funding from the European Union's Horizon 2020 research and innovation programme under the Marie Sklodowska-Curie grant agreement No 813261 and is part of the ABC-EU-XVA project.

Conflicts of interests

The authors have no relevant financial or non-financial interests to disclose.

Data availability

All data generated or analysed during this study are included in this published article. In particular the code to produce the numerical experiments is available at https://github.com/kevinkamm/CIR-.

References

[1] Baker, H., Chen, L., Huang, R., Ravid, S., Stoll, H., of Business, L. N. S. S., and Center, N. Y. U. S. *Stochastic Mean and Stochastic Volatility: A Three-factor Model of the Term Structure of Interest Rates and Its Applications in Derivatives Pricing and Risk Management.* No. Bd. 5 in Competitive Trading of NYSE Listed Stocks: Measurement and Interpretation of Trading Costs. Blackwell Publishers, 1996.

[2] Björk, T. *Arbitrage Theory in Continuous Time.* Oxford Finance Series. Oxford University Press, Incorporated, 2004.

[3] Brigo, D., and El-Bachir, N. Credit derivatives pricing with a smile-extended jump stochastic intensity model. *Derivatives* (2006).

[4] Brigo, D., and Mercurio, F. A deterministic-shift extension of analytically tractable and time-homogeneous short rate models. *Finance and Stochastics 5* (2001), 369 – 388.

[5] Brigo, D., and Mercurio, F. *Interest rate models: theory and practice: with smile, inflation and credit.* Springer, 2006.

[6] Cox, J. C., Ingersoll, J. E., and Ross, S. A. A re-examination of traditional hypotheses about the term structure of interest rates. *The Journal of Finance 36*, 4 (1981), 769–799.

[7] Cox, J. C., Ingersoll, J. E., and Ross, S. A. A theory of the term structure of interest rates. *Econometrica 53*, 2 (1985), 385–407.

[8] Dereich, S., Neuenkirch, A., and Szpruch, L. An euler-type method for the strong approximation of the cox-ingersoll-ross process. *Proceedings of the Royal Society A: Mathematical, Physical and Engineering Sciences 468*, 2140 (2012), 1105–1115.

[9] Francesco, M. A general gaussian interest rate model consistent with the current term structure. *ISRN Probability and Statistics 2012* (09 2012).

[10] Gilli, M., Maringer, D., and Schumann, E. *Numerical Methods and Optimization in Finance*, 1 ed. Elsevier, 2011.

[11] Hull, J. *Options, futures, and other derivatives*, 8. ed., pearson internat. ed ed. Pearson Prentice Hall, 2006.

[12] Hull, J., and White, A. Pricing interest-rate-derivative securities. *Review of Financial Studies 3* (1990), 573–592.

[13] Jamshidian, F. An analysis of american options. *Review of futures markets* (1990).

[14] Jeanblanc, M., Yor, M., and Chesney, M. *Mathematical Methods for Financial Markets.* Springer Finance. Springer London, 2009.

[15] Maghsoodi, Y. Solution of the extended cir term structure and bond option valuation. *Mathematical Finance 6*, 1 (1996), 89–109.

[16] Mercurio, F., and Pallavicini, A. Mixing gaussian models to price cms derivatives. *SSRN Electronic Journal* (2005).

[17] Merton, R. C. Theory of rational option pricing. *The Bell Journal of Economics and Management Science 4*, 1 (1973), 141–183.

[18] Miron, P., and Swannell, P. *Pricing and Hedging Swaps.* Euromoney books. Euromoney Books, 1991.

[19] Orlando, G., Mininni, R. M., and Bufalo, M. A new approach to forecast market interest rates through the CIR model. *Studies in Economics and Finance 37*, 2 (September 2019), 267–292.

[20] Orlando, G., Mininni, R. M., and Bufalo, M. Interest rates calibration with a cir model. *Journal of Risk Finance 20*, 4 (2019), 370–387.

[21] Orlando, G., Mininni, R. M., and Bufalo, M. Forecasting interest rates through vasicek and cir models: A partitioning approach. *Journal of Forecasting 39*, 4 (2020), 569–579.

[22] Pascucci, A. *PDE and martingale methods in option pricing*, vol. 2 of *Bocconi & Springer Series.* Springer, Milan; Bocconi University Press, Milan, 2011.

[23] Vasicek, O. An equilibrium characterization of the term structure. *Journal of Financial Economics 5*, 2 (1977), 177–188.